geoconvention
Calgary • Canada • May 12-14 2025

# Feasibility of 4D frequency domain FWI configured for time-lapse VSP monitoring

*Jinji Li, Kimberly Pike, Kristopher A. Innanen, and Kevin Hall*
*CREWES, University of Calgary*

## Summary

Time-lapse full waveform inversion (FWI) is a critical tool in energy transition, especially for monitoring $CO_2$ storage in geological formations. As part of the Containment and Monitoring Institute (CaMI) Field Research Station (FRS) initiative by Carbon Management Canada (CMC), this research focuses on validating 4D seismic monitoring techniques for carbon capture and storage (CCS) applications. The study involves synthetic tests for 4D acoustic FWI monitoring, using the Snowflake survey methodology, which incorporates both walk-away and walk-around vertical seismic profile (VSP) acquisition strategies. The study begins with an overview of a re-analyzed well log from CaMI, followed by the synthetic models used in the testing. We perform 3D baseline FWI models using acquisition geometry and well log information of the Snowflake dataset and then proceed with a monitor test. The result indicates that 4D FWI is promising for monitoring the $CO_2$ storage with the Snowflake dataset, further providing valuable insights into optimizing source acquisition strategies, aiming to minimize environmental impact while ensuring effective detection of $CO_2$ migration in subsurface reservoirs.

## Theory / Method / Workflow

In the frequency domain, the FWI problem is formulated as follows:

$$argmin_{\boldsymbol{m}}\phi(\boldsymbol{m}) = argmin_{\boldsymbol{m}}\sum_{j=1}^{N_\omega}\sum_{k=1}^{N_s}\frac{1}{2}\left\|\boldsymbol{R}\boldsymbol{u}_{j,k} - \boldsymbol{d}_{j,k}\right\|_2^2, \tag{1}$$

where $\boldsymbol{m}$ represents the inversion variables, $\boldsymbol{R}$ is the sampling matrix capturing receiver measurements, $\boldsymbol{u}$ denotes the discretized wave field produced by a fixed source, and $\boldsymbol{d}$ is the vector of observed data for a given source-receiver pair. We assume a single source and frequency component in the wavefield for simplicity.

The gradient denoting the steepest descent direction of the cost function is computed using the adjoint state method (e.g., Plessix, 2006), which involves correlating the forward and backward propagated wavefields. The backward-propagated wavefield is sourced by the residual wavefield at the receiver locations. The derivative of the objective function with respect to the model parameters is then expressed as:

$$\boldsymbol{g} = \frac{\partial\phi}{\partial\boldsymbol{m}} = Real[\omega^2 f(\omega)G(\boldsymbol{x},\boldsymbol{x}_s,\omega)G(\boldsymbol{x}_r,\boldsymbol{x},\omega)\Delta\boldsymbol{d}^*], \tag{2}$$

where the capital $G$ functions are Green's functions for the source and receiver sides, respectively, and $\boldsymbol{d}^*$ represents the complex conjugate of the data residual. After computing the gradient, a line search is conducted to determine the appropriate step length for updating the model. Thus, the new model update is:

$$\boldsymbol{m}_{new} = \boldsymbol{m} + \alpha \Delta \boldsymbol{m}. \quad (3)$$

## Results

At the CaMI site, Carbon Management Canada (CMC) has injected multiple tons of $CO_2$ into the Basal Belly River Sandstone (BBRS) Formation at a depth of 300 meters. This injection mimics potential $CO_2$ leakage from a large-scale, deep underground storage project. The process is monitored using a combination of geophysical and geochemical monitoring techniques. Based on rock physics models developed by CMC, the changes in $CO_2$ saturation following the injection of 60 tons of $CO_2$ are presented in Figure 1. The figure illustrates a range of saturation gradients, with values starting at 30% close to the injection well and decreasing to 5% at greater distances from the injection point. This gradient provides insight into how $CO_2$ disperses and the efficiency of its injection throughout the modeled region.

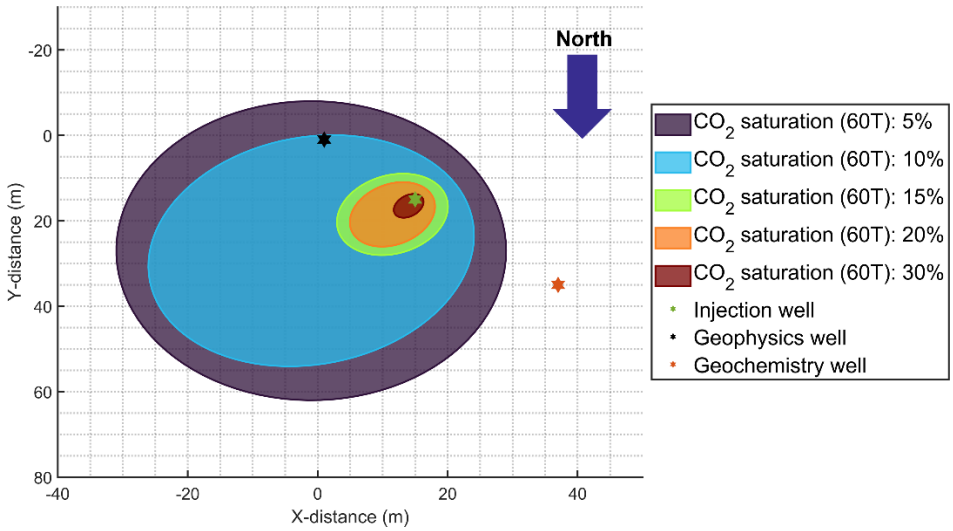


Figure 1. $CO_2$ saturation around the injection well. Colors demonstrate saturation values. Stars of different colors show the injection, geophysics, and geochemistry wells. (0, 0) denotes the location of the geophysics well.

The $CO_2$ concentration at the site follows a distinct directional pattern, emphasizing the necessity for 3D full waveform inversion (FWI) to precisely capture the azimuthal variations in P-wave velocity over time. We revisit the processed data from the CaMI site (Isaac and Lawton, 2016), utilizing the original information and lithological details to construct a model suited for FWI applications. For each lithology, we apply compounded median filters (Leaney and Ulrych, 1987), followed by resampling to 5-meter intervals to preserve lithological information. Finally, a slight smoothing is applied to produce a 1D dataset suitable for FWI. The well log used in this study is shown in Figure 2. The baseline model is built using artificial 1D data as a background, combined with the reservoir simulations made by Macquet et al. (2019), Macquet et al. (2021), Macquet et al. (2022), Kolkman-Quinn et al. 2023. Figure 3 provides a 3D representation of the initial, baseline, and monitor models, along with depth slices at 295 meters.

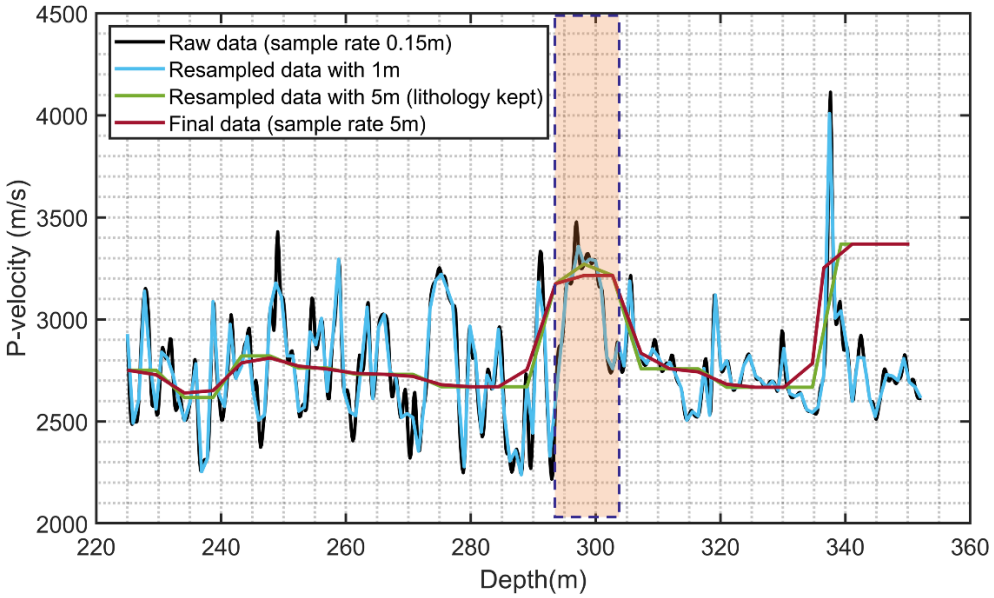


Figure 2. Original and revised P-wave velocity logs.

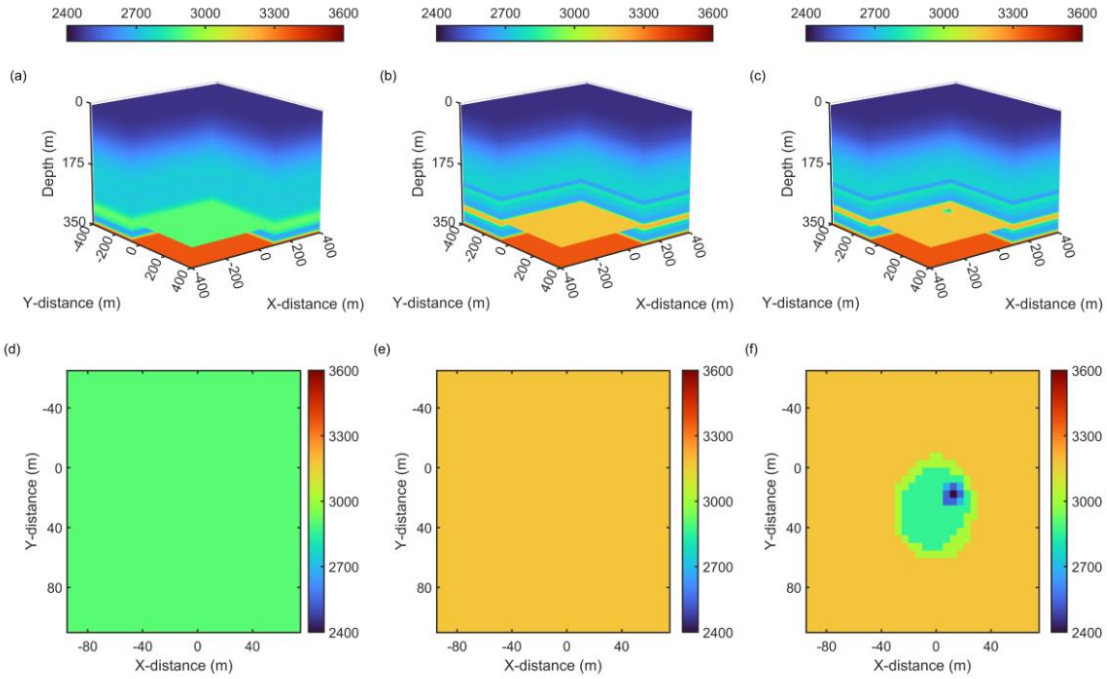


Figure 3. Initial, baseline, and monitor models. (a)-(c) Initial, baseline, and monitor models used in FWI. (d)-(f) Depth slice at 295 meters from initial, baseline, and monitor models.

Figure 4 presents the full source configuration in the Snowflake data. For monitor inversion, we use the frequency of 5-45 Hz, and the monitor result is shown in Figure 5. Detailed plume migration can be depicted by FWI. However, further tests are needed to test the impact of different strategies and acquisitions.

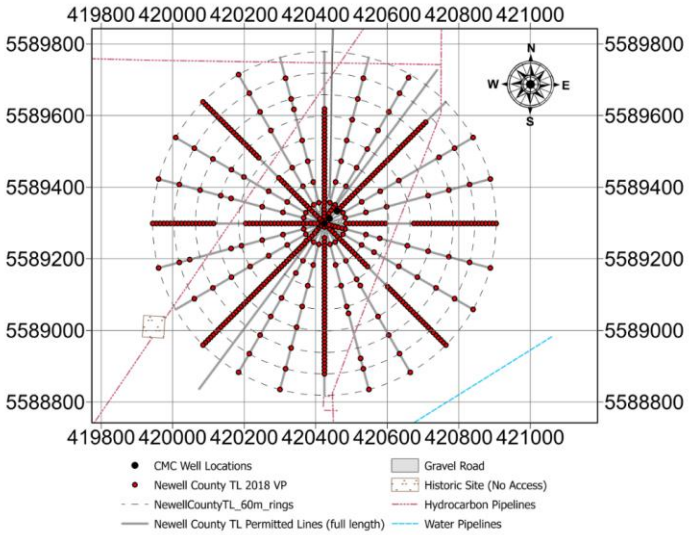


Figure 4. Surface source acquisition of the Snowflake data.

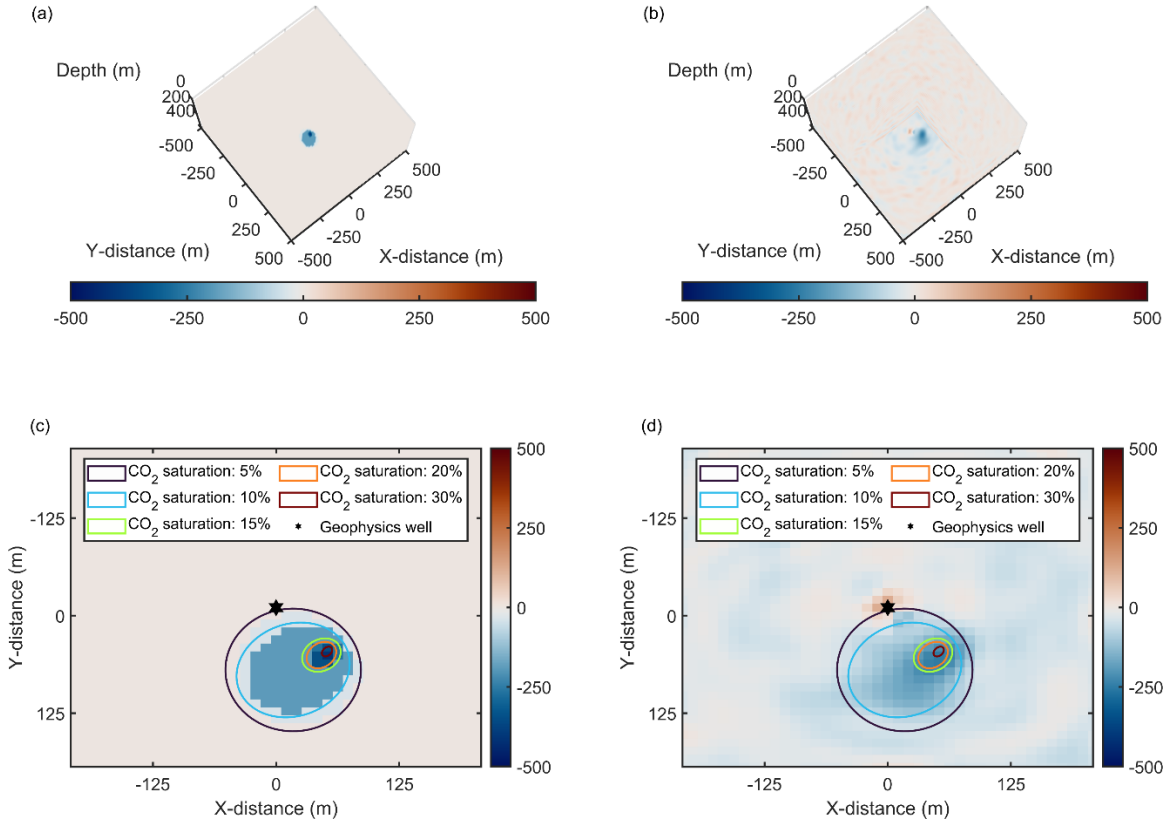


Figure 5. True and estimated time-lapse variations with parallel strategy. (a) 3D view of the true time-lapse variation. (b) 3D view of the estimated time-lapse variation. (c) Zoomed true time-lapse variation in depth of 295 meters. (d) Zoomed estimated time-lapse variation in depth of 295 meters.

## Acknowledgements

The sponsors of CREWES are gratefully thanked for continued support. This work was funded by CREWES industrial sponsors, and NSERC (Natural Science and Engineering Research Council of Canada) through the grant CRDPJ 543578-19. Further support of this work was provided by Emissions Reduction Alberta through the ACT4-SPARSE project.

The Snowflake II data was acquired in collaboration with Carbon Management Canada and several industrial partners at the Newell County Field Research Station. We specially thank Dr. Marie Macquet for sharing the rock physics data.

### References

Isaac, J. H., and Lawton, D. C., 2016, Brooks revisited, CREWES Research Report, 28, 33, 10.

Kolkman-Quinn, B., Lawton, D. C., & Macquet, M. (2023). CO2 leak detection threshold using vertical seismic profiles. International Journal of Greenhouse Gas Control, 123, 103839.

Leaney, W. S., and Ulrych, T. J., 1987, Compound median filtering applied to sonic logs: SEG Technical Program Expanded Abstracts.

Macquet, M., Lawton, D. C., Saeedfar, A., and Osadetz, K. G., 2019, A feasibility study for detection thresholds of $CO_2$ at shallow depths at the CaMI field research station, Newell County, Alberta, Canada: Petroleum Geoscience, 25, No. 4, 509–518.

Macquet, M., Lawton, D. C., Rippe, D., & Schmidt-Hattenberger, C. (2021, September). Semi-continuous electrical resistivity tomography monitoring for CO2 injection at the CaMI Field Research Station, Newell County, Alberta, Canada. In First International Meeting for Applied Geoscience & Energy (pp. 362-366).

Macquet, M., Lawton, D., Osadetz, K., Maidment, G., Bertram, M., Hall, K., ... & Wang, Y. (2022). Overview of Carbon Management Canada's pilot-scale CO2 injection site for developing and testing monitoring technologies for carbon capture and storage, and methane detection. CSEG Recorder, 47(1), 27.

Plessix, R.-E., 2006, A review of the adjoint-state method for computing the gradient of a functional with geophysical applications: Geophysical Journal International, 167, No. 2, 495–503.